

Chapter 8 Seismicity

Chapter 8 Seismicity

CHAPTER 8 SEISMICITY

Contents

8.1	Seismicity in Costa Rica.....	8-1
8.1.1	Outline.....	8-1
8.1.2	Seismic Activity in and around Costa Rica.....	8-1
8.2	Seismic Evaluation for Los Llanos Project Site.....	8-2
8.2.1	Historical Earthquakes around Los Llanos Project Site.....	8-2
8.2.2	Seismic Risk Analysis Based on Stochastic Technique.....	8-2
8.2.3	Maximum Acceleration Estimated for Los Llanos Project Site.....	8-7
8.2.4	Design Horizontal Seismic Coefficient.....	8-7
8.3	Afterword.....	8-9

List of Figures

- Fig. 8-1 Seismo-tectonics in Central-South America
- Fig. 8-2 Seismicity around Costa Rica during 1904-1992
- Fig. 8-3 Historical Earthquakes in the Vicinity of Los Llanos Project Site
- Fig. 8-4 Seismic Risk Analysis Techniques
(Stochastic Technique and Deterministic Technique)
- Fig. 8-5 Return Period for Maximum Acceleration calculated by Eq. (1)
- Fig. 8-6 Return Period for Maximum Acceleration calculated by Eq. (2)
- Fig. 8-7 Return Period by Maximum Acceleration calculated by Eq. (3)
- Fig. 8-8 Return Period by Maximum Acceleration calculated by Eq. (4)
- Fig. 8-9 General Procedure of Earthquake Resistant Design for Dam

List of Tables

- Table 8-1 Recent Earthquake Disasters in Costa Rica
- Table 8-2 Seismicity in Los Llanos Project Area
($M \geq 5.5$, $D \leq 200$ km)
- Table 8-3 Historical Earthquakes in the Vicinity of Los Llanos Project Site
- Table 8-4 Annual Number of Earthquakes during 1904-1992
($D \leq 1,000$ km, D : Epicentral Distance)
- Table 8-5 Distribution of Magnitude and Epicentral Distance of Earthquakes during 1904-1992
- Table 8-6 Annual Maximum Accelerations during 1904-1992
- Table 8-7 Maximum Accelerations for Six Return Periods

Chapter 8 Seismicity

8.1 Seismicity in Costa Rica

8.1.1 Outline

Costa Rica is located on the Circum-Pacific Seismic Belt, and has suffered earthquake disasters many times in the past. Recent typical cases of earthquake disaster are as given in Table 8-1.

Since Costa Rica is situated in a natural environment of high seismic activity in this way, it is essential that thorough evaluation be made regarding earthquakes and proper considerations be given in the earthquake resistant design of electric power facilities.

Here, the seismic risk analysis based on the stochastic technique is performed. And the maximum acceleration at the dam site which is absolutely necessary as a fundamental condition in carrying out the earthquake-resistant design is evaluated.

8.1.2 Seismic Activity in and around Costa Rica

(1) Seismo-tectonics

The Central and South American regions from Mexico to Colombia, Ecuador, and Peru, as shown in Fig. 8-1, comprise a belt of seismic upheavals where the North American Plate, Pacific Plate, Cocos Plate, Caribbean Plate, Nazca Plate, and South American Plate collide against each other in complex manners. The region of Costa Rica on the side of the Pacific Ocean happens to be the boundary where the Cocos Plate sinks under the Caribbean Plate, and many earthquakes have occurred at this plate boundary in the past. Incidentally, the relative moving speed between the Cocos Plate and the Caribbean Plate is approximately 9 cm per year.

(2) Historical Earthquakes

The epicenters of earthquakes which occurred within a radius of 1,000 km from the Los Llanos project site during the period from 1900 to 1992 are shown in Fig. 8-2. As is clear from the figure, the earthquakes have occurred frequently in the Pacific Ocean coastal region along the plate boundary in the vicinity of Costa Rica.

8.2 Seismic Evaluation for Los Llanos Project Site

8.2.1 Historical Earthquakes around Los Llanos Project Site

A list of earthquakes of magnitude 5.5 or greater which have occurred within a radius of 200 km from the Los Llanos project site is given in Table 8-2. This table was made based on the historical earthquake events from the earthquake data files of the NOAA (National Oceanic and Atmospheric Administration) of the National Geophysical Data Center of the United States, etc.

According to the table, the maximum magnitude of earthquakes which have occurred up to now in the surrounding area of Costa Rica was the M_B : 7.7 (real wave magnitude) [December 20, 1904 5hr 44 min 18 sec. focal depth: 60 km, epicentral distance: 164 km]. Of earthquakes of magnitude 5.5 or greater, the closest earthquake to the dam site occurred on March 25, 1990 (13hr 22min 54sec), which had an epicentral distance of 14 km (epicenter: Lat. 9.6°N, Long. 83.9°W, M_B : 6.5).

Further, the historical earthquakes occurring at the Los Llanos project site investigated by Instituto Costarricense Electricidad (ICE) are shown in Table 8-3 and Fig. 8-3.

In this investigation, the earthquakes which had occurred roughly within a radius of 90 km from the project site were picked up. According to the results of this investigation, the maximum magnitude of earthquakes which have occurred in the neighborhood of the Los Llanos project site was the M_s : 7.3 (surface wave magnitude) [(1) April 24, 1916, epicentral distance : 191 km, (2) December 21, 1939, epicentral distance : 81 km]. In Table 8-3, the modes of earthquakes are classified into two types. One is the plate boundary earthquakes, and the other is the inland earthquakes. The plate boundary earthquakes occurred at the plate boundaries. The inland earthquakes occurred in inland areas. From the table, it may be comprehended that the earthquakes in excess of magnitude 7.0 were all plate boundary earthquakes (notation: S).

8.2.2 Seismic Risk Analysis Based on Stochastic Technique

(1) Outline of Analysis

Evaluation techniques for seismic risk analyses, as shown in Fig. 8-4, may be broadly divided into stochastic technique and deterministic technique.

A stochastic technique is a method for estimating the maximum acceleration which may be expected in any return period based on data of historical earthquakes occurred using attenuation models and stochastic models. This technique has good reliability when enough earthquake data are available, and is presently the most generally used method. This technique can be also applied to the seismic risk evaluation based on the earthquake faults by estimating the magnitude from the length of the faults in case the location of the earthquake faults and the length are known.

On the other hand, a deterministic technique is a method for estimating the earthquake motion assumable for the site by numerical analysis setting up the fault models for earthquakes based on the seismic activity (aftershock area, periodicity), distribution of earthquake faults, crustal movements, and on consideration of the underground structure. It is possible with this method to obtain a rational result if the conditions necessary for analyses can be assumed properly. However in general, it is very difficult for estimation of fault parameters or underground structures at present level. Furthermore, the estimation of short-period components (roughly, shorter than 1 sec) cannot be adequately done at the present time. So it is not necessarily a generally-used method for practical purposes, although there are some cases of application for research purposes.

Taking into account the advantages and disadvantages of the analysis techniques described above, it was decided for the seismic risk analysis to be made by a stochastic technique because of plentiful data of historical earthquakes with regard to the Los Llanos project site.

(2) Analysis Method

(i) Gumbel's Extreme Value Theory

Assuming that the stochastic variable x follows the stochastic function $G(X)$:

$$G(x) = Q(X \leq x)$$

The probability that x will be larger than any of X_1, X_2, \dots, X_n is defined as follows:

$$\begin{aligned} P_n(x) &= Q(X_1 \leq X, X_2 \leq X, \dots, X_n \leq X) \\ &= G_n(X) \end{aligned}$$

At this time, the return period $P(x)$ and the conversion variable z will be expressed as follows:

$$P(x) = 1 / \{1 - P_n(x)\}$$
$$Z = -\ln \{1 - P_n(x)\}$$

Gumbel's extreme value theory (1958) can be applied even when the original distribution of the stochastic variable is unknown. But in case of applying the extreme value theory to earthquake phenomena, the frequency of earthquake occurrence, and the return period can be predicted and evaluated if the following hypothetical conditions are satisfied:

- Hypothesis (1) The pattern of earthquake occurrence in the past will continue without failure in the future.
- Hypothesis (2) The maximum earthquake phenomenon observed in the given time interval is an independent phenomena.
- Hypothesis (3) The future trend of occurrence of maximum earthquake in the given time interval is the same as in the past.

In Gumbel's extreme value theory, three kinds of extreme asymptotic distributions are proposed according to the behavior characteristics of maximum value of stochastic variables.

1st Asymptotic Distribution

$$P_n(x) = \exp \{-\exp(-\alpha_n)(x-V)\}$$

2nd Asymptotic Distribution

$$P_n(x) = \exp \{[-(V-\varepsilon)/(x-\varepsilon)]^k\}$$

3rd Asymptotic Distribution

$$P_n(x) = \exp \{[-(W-x)/(W-V)]^k\}$$

There is no upper limit or lower limit for the stochastic variable in the 1st asymptotic distribution. With the 2nd asymptotic distribution, there is a lower limit for stochastic variables, and with the 3rd asymptotic distribution, an upper limit.

Incidentally, the stochastic function of maximum acceleration assumed for the site considered here is unknown. However, since it may be considered that there is an upper limit to the maximum amplitude of earthquake motion at any site, it can be judged to be reasonable to apply the 3rd asymptotic distribution. In the 3rd asymptotic distribution equation, w is the upper limit of maximum amplitude, k is a shape factor, V is the maximum value of characteristic, and x is a random stochastic variable. With A_{max} as the maximum acceleration of earthquake motion at a certain site in a unit period of time, x is expressed by the following equation:

$$x = \log A_{max}$$

And, the plotted location of maximum acceleration in a unit period of time is obtained by the following equation:

$$P(m) = (N - m + 1)/(N + 1)$$

Where, N indicates the number of unit periods for the analysis, and m the order of rank from the maximum value.

(ii) Earthquake Data

In the seismic risk analysis here, the earthquake data from the earthquake data file of NOAA (National Oceanic and Atmospheric Administration of the United States Geophysical Data Center) were used.

The earthquakes occurred within a radius of 1,000 km from the Los Llanos project site during the period from 1900 to 1992 and were 3,886 in number.

A radius of 1,000 km was set here as the object of evaluation, and when the damping characteristics of maximum acceleration of earthquake motion is considered, it is a range which is adequate for evaluation. The numbers of earthquakes which occurred in each year during the period from 1900 to 1992 are given in Table 8-4. The distribution of earthquake magnitudes and epicentral distance used in the stochastic analyses are as shown in Table 8-5.

(ii) Attenuation Model

The equations for attenuation with distance applied in prediction of maximum acceleration were the four below out of those proposed up to the present.

The "A" in each equation depicts maximum acceleration (gal), the "M" magnitude of earthquake, and the "R" hypocentral distance (km).

$$\text{Log } A = 3.090 + 0.347M - 2 \text{ Log } (R+25) \dots\dots\dots (1)$$

Proposed by C. Oliveira

$$\text{Log } A = 2.647 + 0.278 M - 1.301 \text{ Log } (R+25) \dots\dots\dots (2)$$

Proposed by P. K. McGuire

$$\text{Log } A = 2.041 + 0.347 M - 1.6 \text{ Log } R \dots\dots\dots (3)$$

Proposed by L. Esteva and E. Rosenblueth

$$\text{Log } A = 2.308 + 0.411 M - 1.637 \text{ Log } (R+30) \dots\dots\dots (4)$$

Proposed by T. Katayama

(3) Analysis Results

The data of 3,886 earthquakes during the 93-year period from 1900 to 1992 were used for prediction of maximum acceleration by stochastic analysis. Here, the isochronal interval of the probability model based on the "Gumbel's extreme value theory" was taken as 1 year. Although the probability relationship of maximum acceleration expected at the Los Llanos project site is unknown, since it is logical to consider that there is an upper limit to the value of maximum acceleration at the site, as previously stated, a third asymptotic distribution was assumed.

Regarding the maximum accelerations of the Los Llanos project site evaluated using the equations of Oliveira, McGuire, Esteva-Rosenblueth, and Katayama, the largest maximum acceleration values evaluated for each of the 93 years from 1900 to 1992 are given in Table 8-6.

The analytical results of maximum accelerations for the return periods are shown in Fig. 8-5 (Oliveira's equation), Fig. 8-6 (McGuire's equation), Fig. 8-7 (Esteva-Rosenblueth's equation), and Fig. 8-8 (Katayama's equation).

8.2.3 Maximum Acceleration Estimated for Los Llanos Project Site

The results of stochastically estimating the maximum accelerations at the Los Llanos project site for return periods of 50, 100, 200, 500, 1,000, and 10,000 years applying the equations of Oliveira, McGuire, Esteva-Rosenblueth, and Katayama based on historical earthquakes are shown in Table 8-7.

The evaluation results based on McGuire's and Katayama's equations, indicate larger maximum accelerations compared with those based on Oliveira's and Esteva-Rosenblueth's equations. It is thought these differences resulted because the earthquake data which served as the basis from which the attenuation model was derived depended on the ground conditions of the site.

In other words, Oliveira's equation was proposed based on earthquake data obtained at the surface of hard bedrock. As for the equation of Esteva-Rosenblueth, an equation for the surface of hard ground was modified into an equation for the surface of bedrock and proposed.

On the other hand, McGuire's equation and Katayama's equation were based on earthquake data obtained at the surfaces of various kinds of ground from hard to soft. Because of this, McGuire's and Katayama's equations tend to give maximum accelerations of larger values compared with Oliveira's and Esteva-Rosenblueth's equations.

In this way, the results will be different depending on the attenuation model applied. With regard to the Los Llanos project site, it can be judged that because of the seismic activity of Costa Rica being fundamentally high, it will be appropriate to assume a value enveloping the results obtained here, that is, "300 gal."

This value of 300 gal corresponds roughly to a return period of 10,000 years from the standpoint of stochastic analysis results.

8.2.4 Design Horizontal Seismic Coefficient

(1) Design Horizontal Seismic Coefficient of Ground

Regarding the relationship between the maximum horizontal acceleration of earthquake motion and the design horizontal seismic coefficient, the following equation will generally be valid:

$$K_h = R \frac{A_{max}}{980} \dots\dots\dots (5)$$

- where, K_h : Design horizontal seismic coefficient
 R : Conversion factor
 A_{max} : Maximum horizontal acceleration of earthquake motion (gal)

The design horizontal seismic coefficient of the above equation is what is called effective seismic coefficient or equivalent seismic coefficient, and the following proposals have been made in research in Japan.

$$(1) K_h = (0.35 \sim 0.42) A_{max}/980 \text{ (effective value of steady sine wave)} \dots\dots\dots (6)$$

$$(2) K_h = 0.33 (A_{max}/980)^{1/3} \text{ (Noda}^4, 1975) \dots\dots\dots (7)$$

$$(3) K_h = 0.072 + 0.332 (A_{max}/980) \text{ (Matsuo}^5, 1984) \dots\dots\dots (8)$$

$$(4) K_h = (0.13 \sim 0.34) A_{max}/980 \text{ (Hakuno}^6, 1984) \dots\dots\dots (9)$$

$$(5) K_h = (0.50 \sim 0.60) A_{max}/980 \text{ (Watanabe}^7, 1984) \dots\dots\dots (10)$$

In the Technical Guideline for Aseismic Design of Nuclear Power Plants⁸⁾ published in 1987, the following equation is proposed as a result of overall evaluation and consideration taking into account these cases of study.

$$K_h = (0.40 \sim 0.60) A_{max}/980 \dots\dots\dots (11)$$

The concept of effective seismic coefficient (equivalent seismic coefficient) was derived so that the largeness of stresses produced in ground and structures by earthquake motions will be equivalent for cases of handling dynamically (dynamic analysis by input of earthquake motion) and for cases of handling statically (static analysis using design seismic coefficient). The conversion factor which will be required for calculating effective seismic coefficient (equivalent seismic coefficient) is thought to be largely dependent on the frequency characteristics of design input earthquake motions and wave motion impedance of foundation rock (shearing wave velocity x density). That is, for an earthquake motion with long-period components predominant, a large value (for example; 0.6) should be taken for the conversion factor. And for an earthquake motion with short-period components predominant, a small value (for example; 0.4) can be taken for the conversion factor.

In case the wave motion impedance of foundation rock is small, the conversion factor should be small (0.4 for example). On the other hand, in case the impedance is large, the conversion factor should be large (0.6 for example).

Applying Eq. (5) and supposing $R = 0.5$, the design ground horizontal seismic coefficient for the Los Llanos project site can be estimated to be $K_h = 0.15$, since the maximum acceleration at the site is 300 gal.

(2) Design Horizontal Seismic Coefficient for Dam

Regarding the design horizontal seismic coefficient for dam, as shown below, the same value as the design horizontal seismic coefficient of ground is adopted for fill dam and gravity dam. For arch dam, a value twice the design horizontal seismic coefficient of ground is adopted.

Dam Type	Design Horizontal Seismic Coefficient
Fill Dam	0.15
Gravity Dam	0.15
Arch Dam	0.30

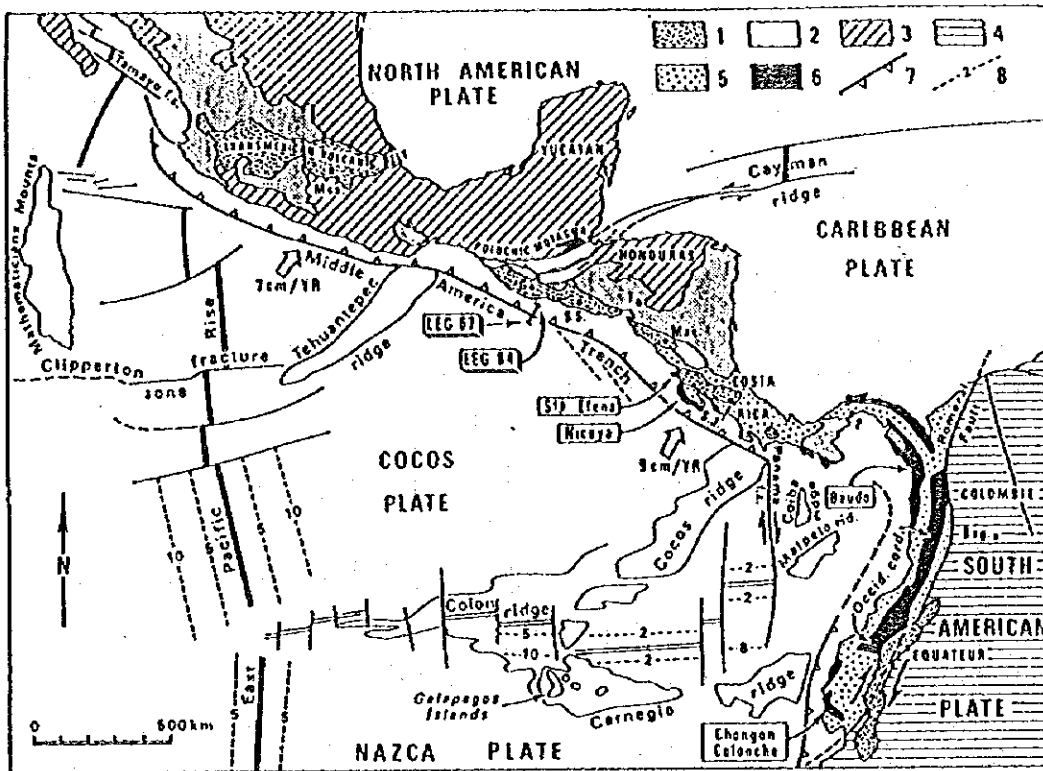
8.3 Afterword

The determination of optimum configuration and cross section of dam, and the basic stability evaluation of dam during earthquake are normally made according to the seismic coefficient method. The design seismic coefficient to be used in the seismic coefficient method, as previously mentioned, is evaluated considering a conversion factor for the maximum acceleration of earthquake motion assumed for the site. The value of the conversion factor can be thought to depend on the frequency characteristics of the earthquake motions assumed, and the dynamic characteristics of dam and foundation rock to be considered in the earthquake-resistant design. Therefore, it is desirable for the seismic stability of dam to be ascertained by dynamic analyses. The appropriateness of the design seismic coefficient can be verified by comparison of dynamic and static analyses.

For the reference, general procedure of earthquake resistant design for dams is shown in Fig. 8-9.

Reference

- 1) Vasconez K.C.; Costa Rica : A Country profile, V.S. Department of Commerce Report, No. PB-89-105829.
- 2) Bourgeois J, J. Azema, J. Tournon, J. Aubouin,
The geological history of the Caribbean-Cocos plate boundary with special reference to the Nicoya ophiolite complex (Costa Rica) and D.S.D.P. results (Legs 67 and 84 off Guatemala) :
A synthesis, Tectonophysics, Vol.108, pp1-32, 1984.
- 3) Instituto Costarricense de Electricidad
P.H. LOS LLANOS Estudio Seismologico Preliminar, Noviembre 1989.
- 4) Noda, S., Kambe, T., and Chiba, T., "Seismic Coefficient of Gravity-type Quaywall and Ground Acceleration," Report of Port and Harbour Technical Research Institute, Ministry of Transport, Vol. 14, No. 4, PP.67-111, 1975
- 5) Matsuo, M., and Itabashi, K., "Study on Evaluation of Aseismicity of Slopes and Soil Structures," Transactions of the Japan Society of Civil Engineers, No. 352, III-2, Dec. 1984
- 6) Hakuno, M., and Morikawa, O., "A Simulation Concerning Earthquake Acceleration and Failure of Structures," Transactions of the Japan Society of Civil Engineers, No. 344, I-1, pp.299-302, Apr. 1984
- 7) Watanabe, H., Sato, S., and Murakami, S., "Evaluation of Earthquake-Induced Sliding in Rockfill Dams," Soil and Foundation, Vol. 24, No. 3, pp. 1-14, Sept. 1984
- 8) Japan Electric Association, "Technical Guide to Aseismic Design of Nuclear Power Plants," 1987



Tectonic setting of the Santa Elena and Nicoya Peninsulas (Costa Rica) and of Legs 67 and 84 off Guatemala. Present-day plate motions from Minster and Jordan (1978). 1 = Pliocene and Pleistocene volcanism; 2 = Oligocene and Miocene volcanism; 3 = North American plate; 4 = South American plate; 5 = Cenozoic formations of ophiolitic Andes and southern Central America; 6 = Mesozoic and Cenozoic ophiolitic complexes; 7 = subduction zones; 8 = magnetic anomalies.

Fig. 8-1 Seismo-tectonics in Central-South America

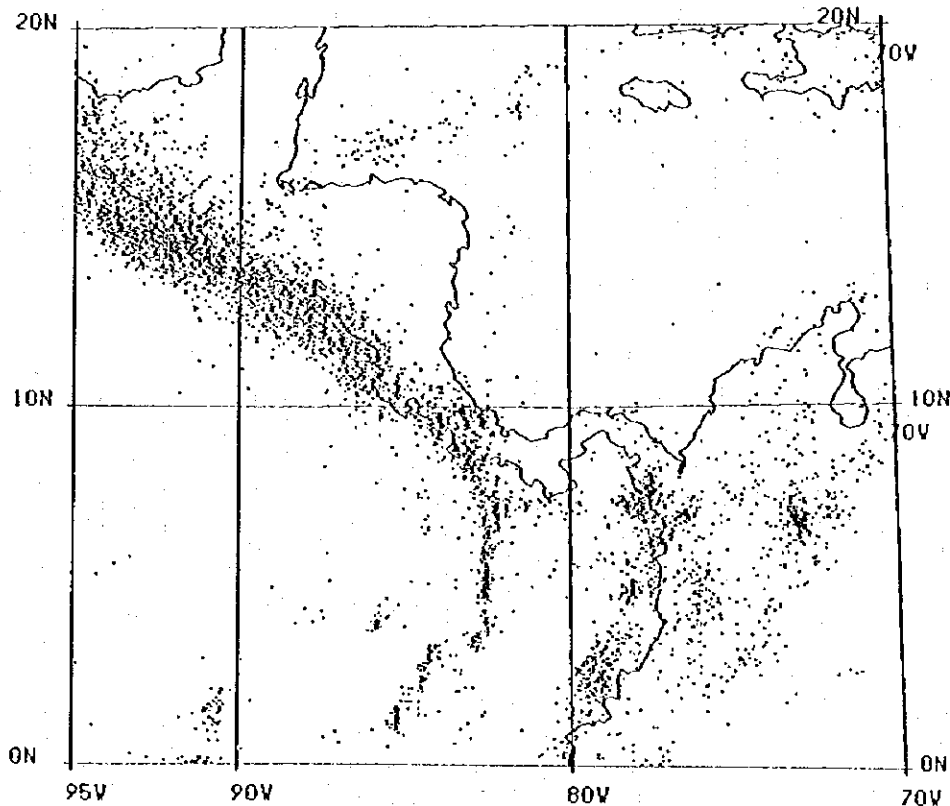


Fig. 8-2 Seismicity around Costa Rica during 1900-1992

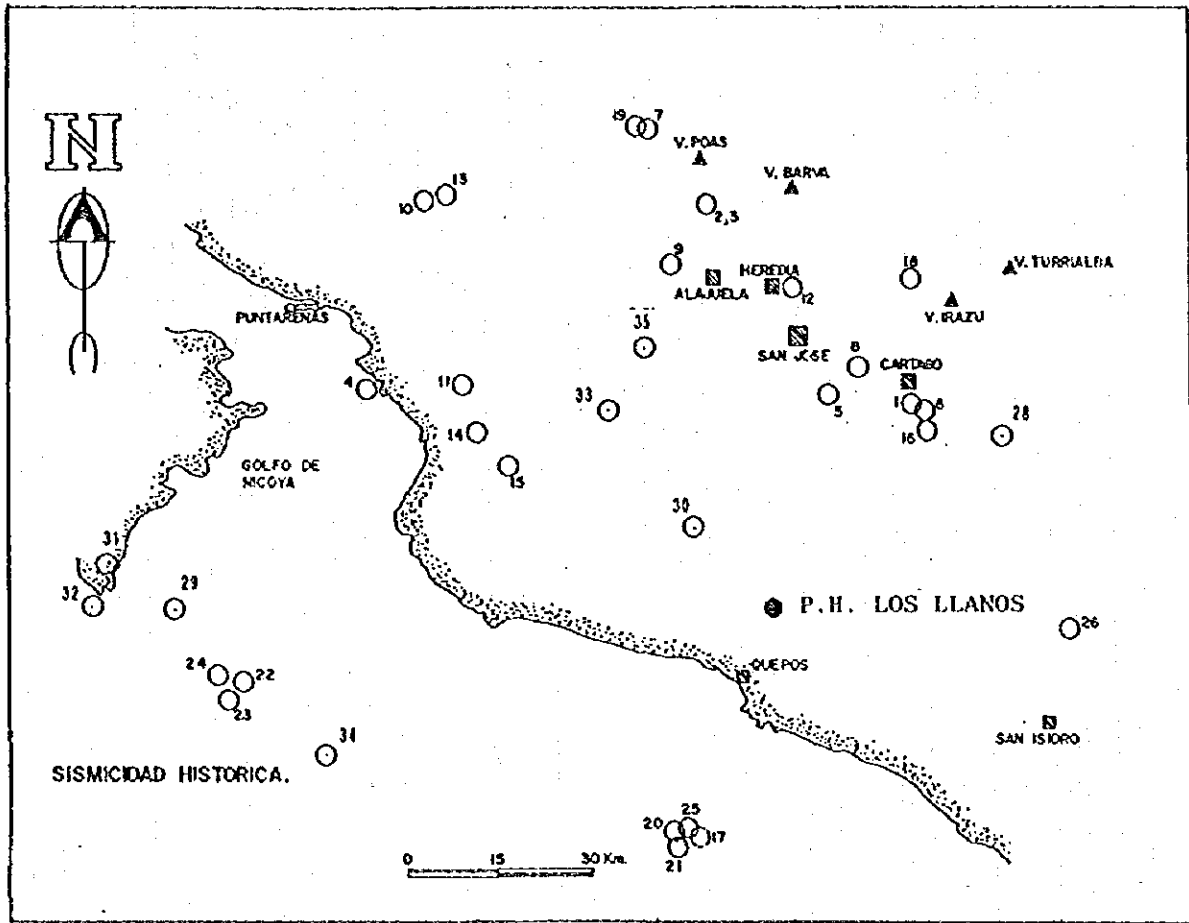


Fig. 8-3 Historical Earthquakes in the Vicinity of Los Llanos Project Site

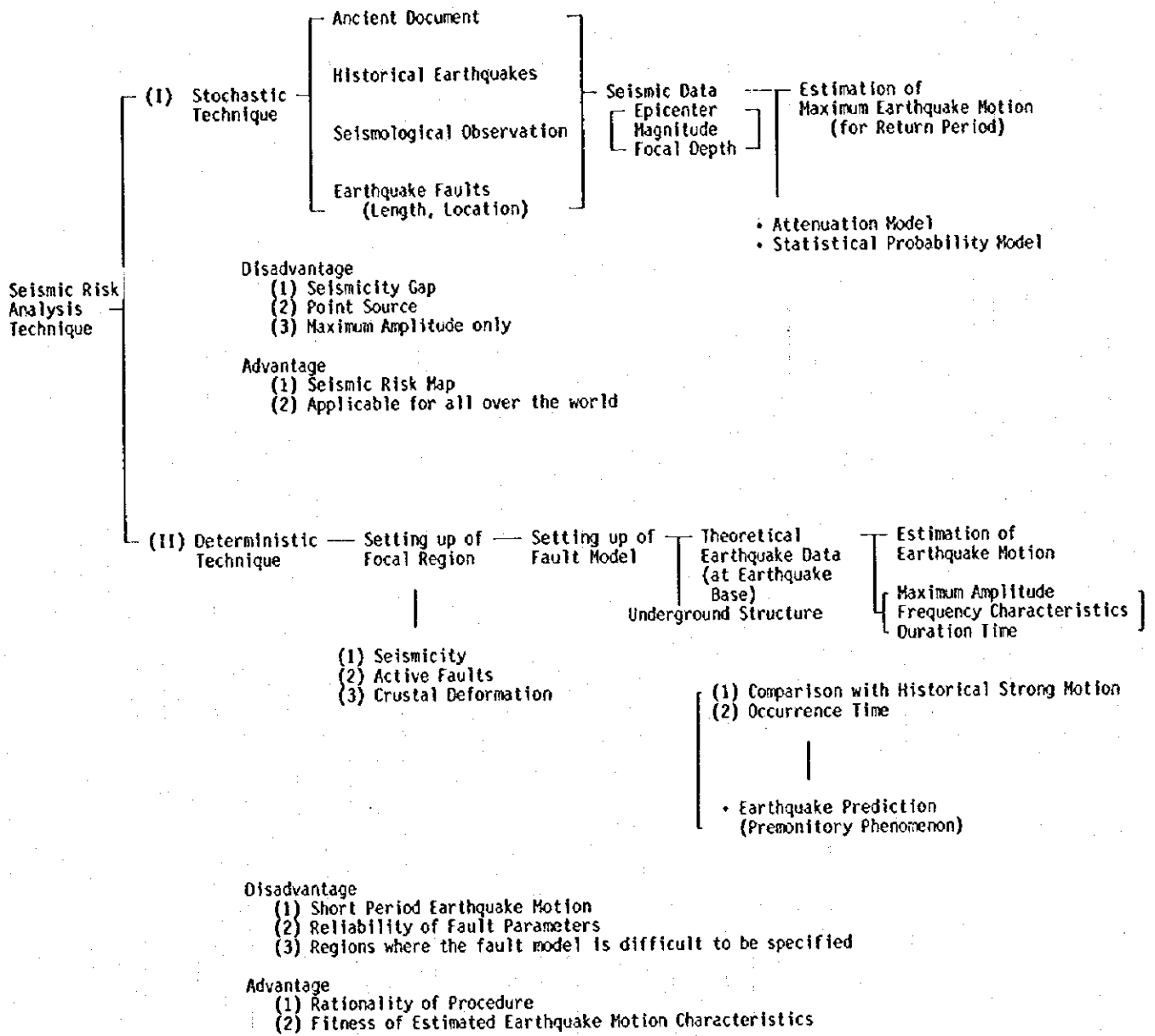
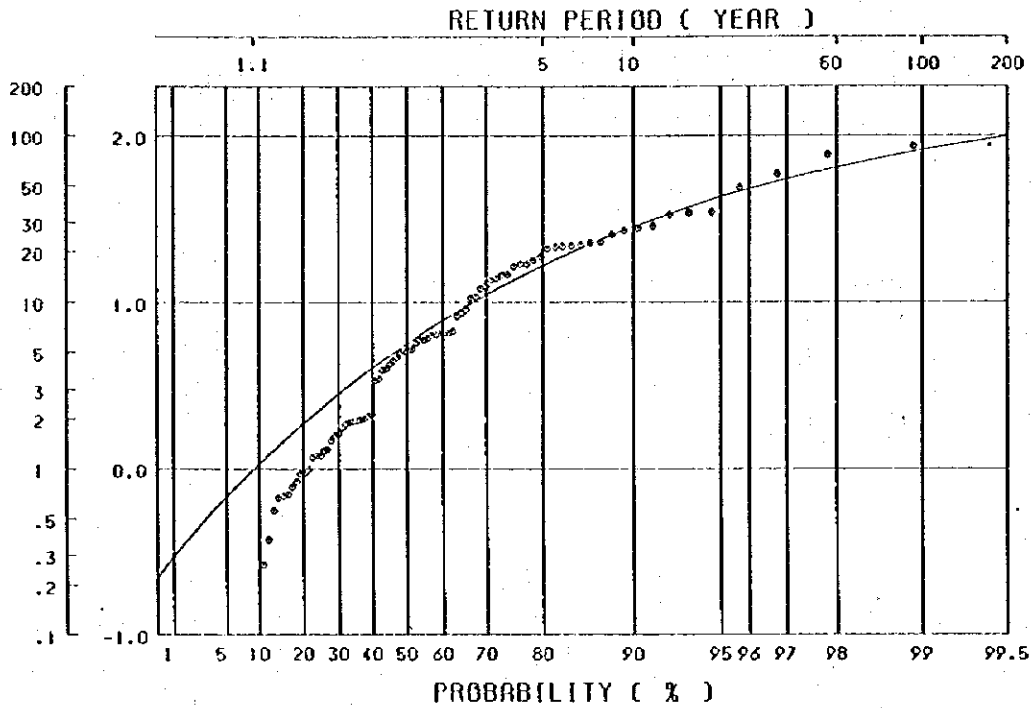


Fig. 8-4 Seismic Risk Analysis Techniques (Stochastic Technique and Deterministic Technique)

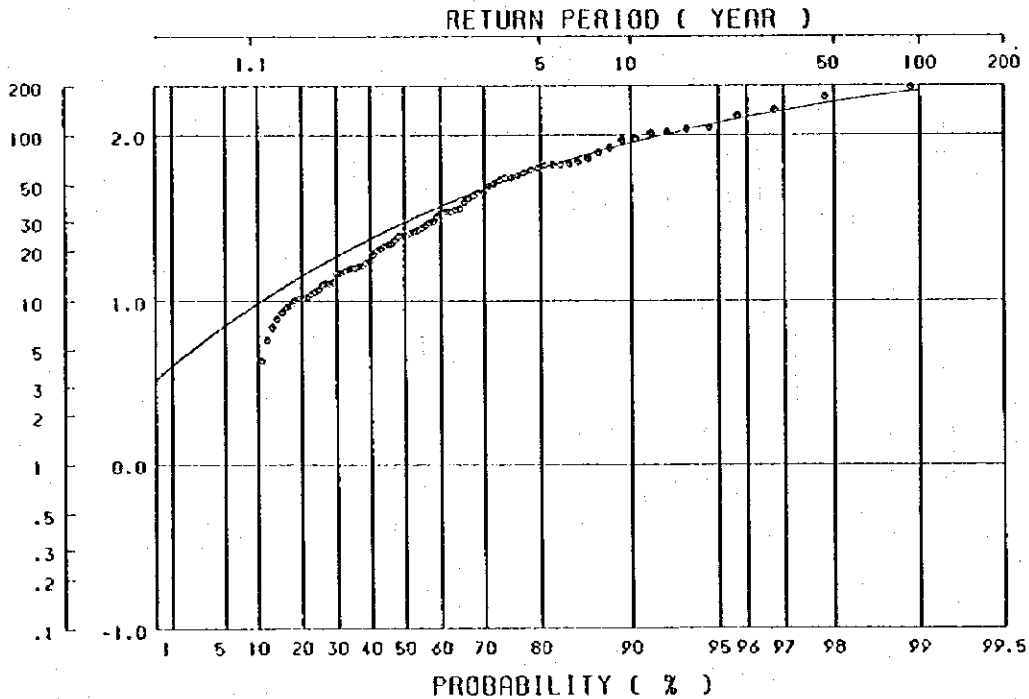
COSTA RICA
LOS LLANOS



1: $\text{LOG } A = 3.09 + 0.347M - 2\text{LOG}(R+25)$ (C. OLIVEIRA)

Fig. 8-5 Return Period for Maximum Acceleration calculated by Eq. (1)

COSTA RICA
LOS LLANOS

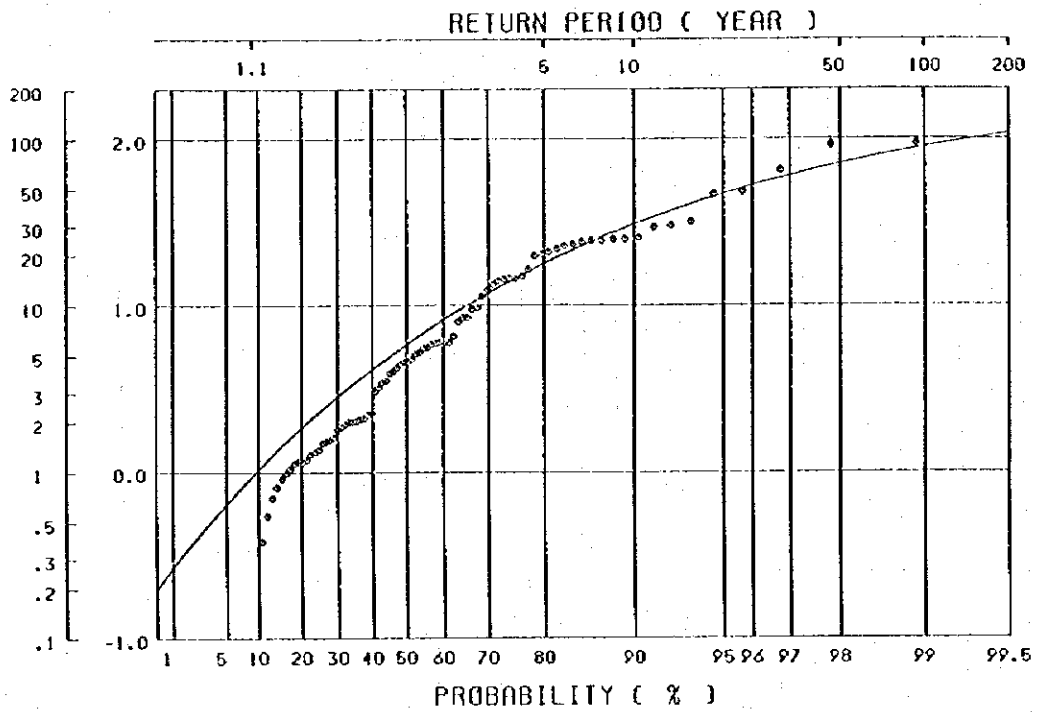


2: $\text{LOG } A = 2.674 + 0.278M - 1.301\text{LOG}(R+25)$

(R.K. MCGUIRE)

Fig. 8-6 Return Period for Maximum Acceleration calculated by Eq. (2)

COSTA RICA
LOS LLANOS

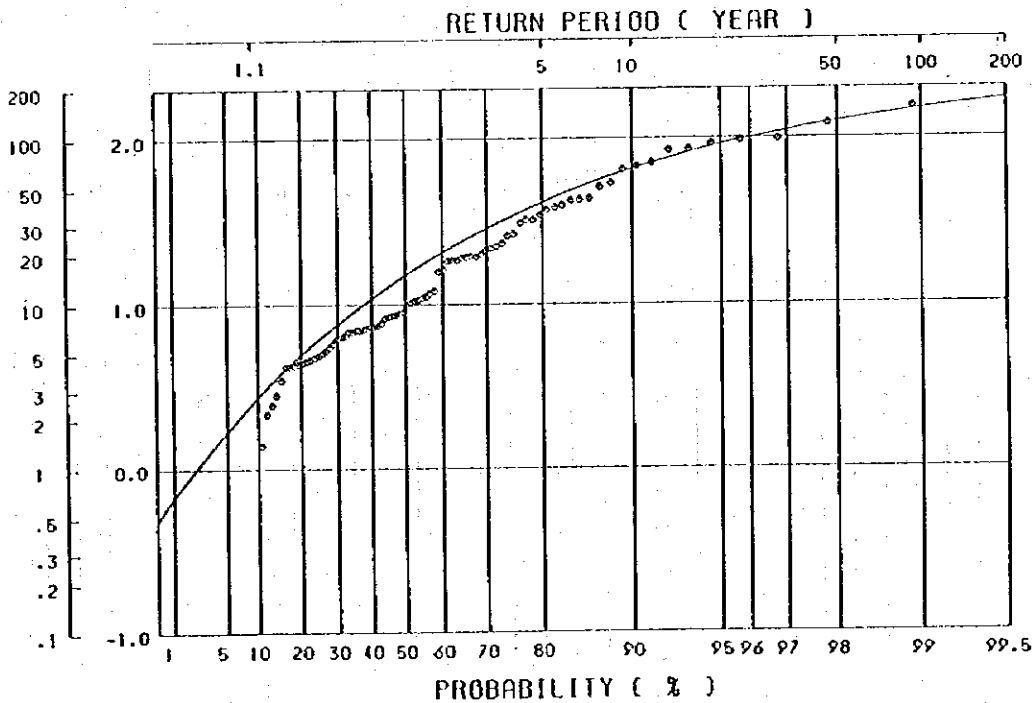


3: $\text{LOG } A = 2.041 + 0.347H - 1.6\text{LOG}(R)$

(L. ESTEVA & E. ROSENBLUETH)

Fig. 8-7 Return Period for Maximum Acceleration calculated by Eq. (3)

COSTA RICA
LOS LLANOS



4: $\text{LOG } A = 2.308 + 0.411H - 1.637\text{LOG}(R+30)$

(T. KATAYAMA)

Fig. 8-8 Return Period for Maximum Acceleration calculated by Eq. (4)

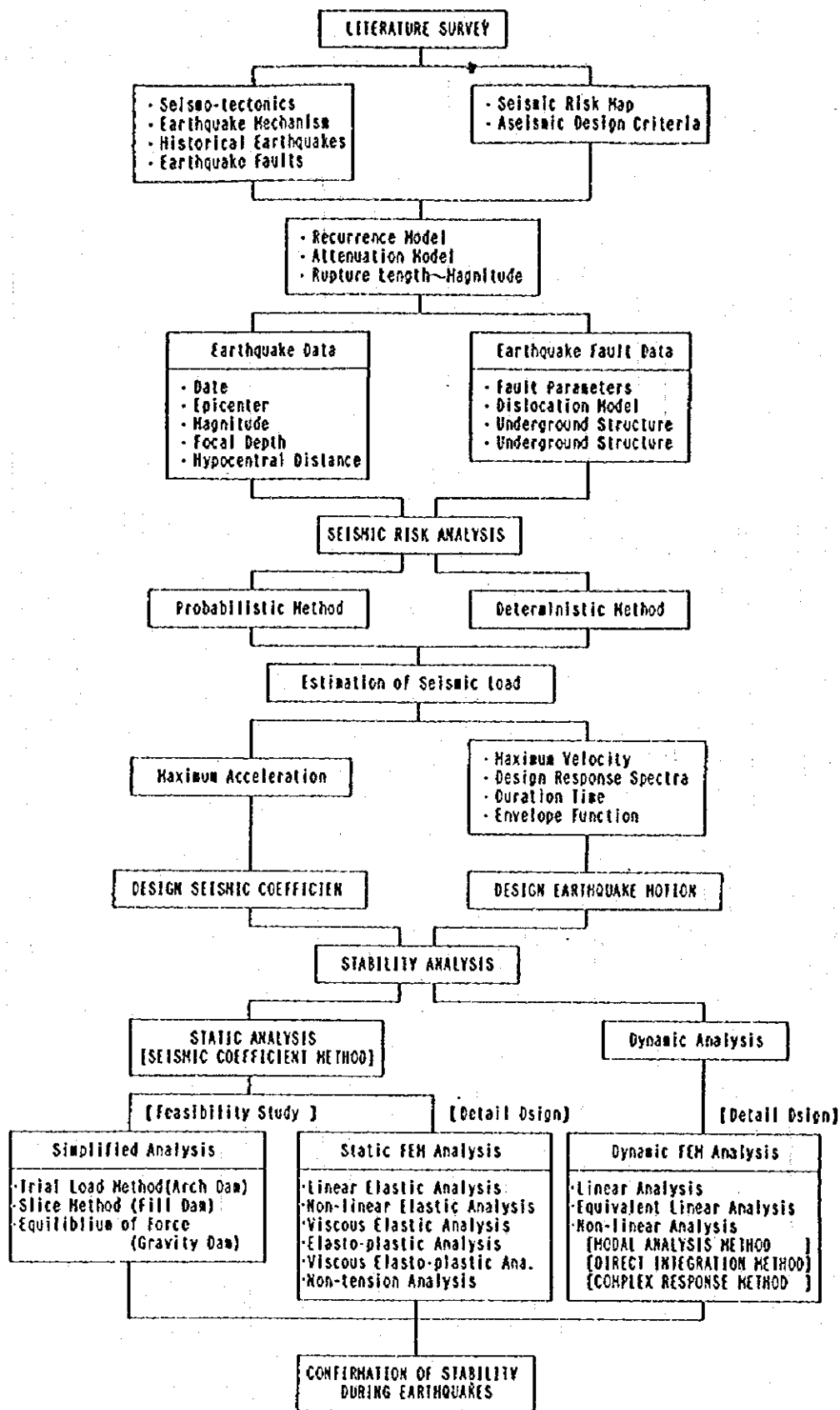


Fig. 8-9 General Procedure of Earthquake Resistant Design for Dam

Table 8-1 Recent Earthquake Disasters in Costa Rica

Earthquake Disaster			Damage		
Date	Type	Location	Killed	Affected	Homeless
04-14-73	Earthquake	S. of Laguna Arenal	21	3,563	84
			Comments: 98 Injured		
04-02-83	Earthquake	SE of San Jose	1	475	475
			Comments: 200 Injured		
07-03-83	Lands lides (due to earthquake)	San Jose Province	1	5,000	0
04-22-91	Earthquake (M=7.0)	SW of Limon (9°36.88'N, 83°9.48'E)	48	6,840	6,752
			Comments: 585 Injured		

Source: OFDA Disaster History on file at the Office of U.S. Foreign Disaster Assistance in Washington, DC. Covers 1900 to the present.

Table 8-2 Seismicity in Pirris Project Area
 $M \geq 5.5$, $D \leq 200$ km

SITE		LONG. = -84.050 LATI. = 9.550					
DATE	TIME	LONGITUDE	LATITUDE	MB	EPD	HPD	DEPTH
18410902	123000	-82.900	9.833	5.8	129.907	133.326	30.000
18510328	131500	-83.183	10.133	5.5	114.855	118.709	30.000
18881230	101200	-83.183	10.133	5.8	114.855	118.709	30.000
19041220	054418	-83.000	8.500	7.7	163.758	174.404	60.000
19050120	182308	-83.667	9.850	6.7	53.542	61.374	30.000
19090816	0658	-84.300	10.000	7.0	56.824	82.638	60.000
19100504	184700	-82.900	9.833	5.5	129.907	133.326	30.000
19110829	40600	-83.300	10.233	5.5	111.685	115.644	30.000
19120606	64000	-83.267	10.017	5.5	100.186	104.581	30.000
19160424	080208	-85.000	11.000	7.3	191.236	200.427	60.000
19160426	22130	-83.617	10.133	7.3	80.124	85.557	30.000
19240304	100742	-83.550	9.850	7.0	64.076	70.751	30.000
19311220	145942	-84.500	11.000	6.1	167.799	326.430	280.000
19360320	184628	-84.000	11.000	6.0	160.476	163.256	30.000
19370309	154020	-83.500	9.000	6.5	85.778	90.873	30.000
19390618	164605	-83.000	10.000	6.6	125.421	143.633	70.000
19390718	164605	-83.100	10.000	6.5	115.430	119.265	30.000
19391221	205447	-83.600	10.133	7.3	81.217	86.580	30.000
19391222	44358	-83.517	9.800	6.7	64.666	71.286	30.000
19401005	143843	-84.200	9.500	6.4	17.371	34.666	30.000
19401027	53537	-83.500	9.750	6.7	64.232	70.892	30.000
19411205	204658	-83.000	8.500	7.2	163.758	166.484	30.000
19411206	012501	-85.200	10.500	6.3	164.147	166.866	30.000
19411206	212440	-84.000	8.500	6.8	116.262	120.070	30.000
19450603	130536	-82.600	8.600	6.9	190.939	193.281	30.000
19481119	10424	-82.500	10.000	7.0	177.081	179.604	30.000
19490818	133325	-83.000	8.500	6.6	163.758	166.484	30.000
19501005	1609	-84.000	11.000	7.7	160.476	163.256	30.000
19520425	0602	-83.200	8.100	6.5	185.610	188.019	30.000
19520513	193145	-85.300	10.300	6.8	160.205	172.516	64.000
19520909	125442	-83.200	9.200	7.0	101.144	105.500	30.000
19521230	120703	-82.900	10.017	5.5	136.228	139.492	30.000
19550901	173303	-83.317	10.233	5.8	110.332	114.338	30.000
19580415	035235	-84.500	8.000	6.8	178.431	180.935	30.000
19560719	232625	-84.500	9.500	6.3	49.647	58.007	30.000
19570408	201809	-83.000	8.500	6.6	163.758	166.484	30.000
19580606	091114	-84.500	8.000	6.7	178.431	180.935	30.000
19610523	0340245	-84.000	9.800	5.9	28.190	97.179	93.000
19660327	1853413	-83.500	8.800	5.9	102.657	110.542	41.000
19660409	24205	-83.167	9.183	5.7	105.248	107.732	23.000
19720207	1914476	-83.884	8.550	5.5	112.106	112.977	14.000
19730414	83400	-83.900	10.450	6.5	100.894	105.260	30.000
19740228	2020102	-84.067	9.350	5.8	22.198	51.076	46.000
19761220	1018568	-83.933	9.283	5.5	32.163	73.420	66.000
19780823	38	-84.300	10.100	7.0	66.726	82.197	48.000
19790824	426	-82.400	9.000	6.5	191.343	194.168	33.000
19830403	0250011	-83.134	8.733	6.5	135.328	140.295	37.000
19830509	155303	-82.967	8.233	5.5	188.132	192.132	39.000
19830703	171423	-82.667	9.500	6.2	151.761	154.697	30.000
19830923	2344302	-83.400	8.433	5.6	142.688	148.741	42.000
19900325	132254	-83.933	9.600	6.5	13.934	28.621	25.000
19900428	123	-82.500	8.883	6.3	185.702	187.121	23.000
19901222	172754	-83.300	9.900	5.7	90.882	90.970	4.000
19910422	100	-83.150	9.617	6.5	98.935	99.439	10.000
19910422	200	-83.150	9.617	7.0	98.935	99.439	10.000
19910424	191258	-82.500	9.433	5.5	170.924	171.344	12.000
19920307	153	-83.317	10.200	6.2	107.840	133.681	79.000

Table 8-3 Historical Earthquakes in the Vicinity of Los Llanos Project Site

No.	Fecha	Lat. N	Long. W.	Mag.	Fuente
01	02/09/1841	09 50.50	83 54.60	M=5.8	F
02	18/03/1851	10 08.00	84 11.70	M=5.5	F
03	30/12/1888	10 08.00	84 11.70	M=5.2	F
04	20/01/1905	09 51.00	84 40.80	Ms=6.7	S
05	13/04/1910	09 50.10	84 01.60	M=5.2	F
06	04/05/1910	09 50.50	83 54.60	M=5.5	F
07	29/08/1911	10 14.00	84 18.00	M=5.5	F
08	21/02/1912	09 52.00	84 00.00	M=5.0	F
09	06/06/1912	10 01.50	84 16.50	M=5.5	F
10	24/04/1916	10 08.40	84 37.80	Ms=7.3	S
11	04/03/1924	09 51.00	84 33.60	Ms=7.0	S
12	18/06/1939	10 00.00	84 06.00	Ms=6.5	F
13	21/12/1939	10 08.40	84 36.00	Ms=7.3	S
14	22/12/1939	09 48.00	84 31.80	Ms=6.7	S
15	27/10/1940	09 45.00	84 30.00	Ms=6.7	S
16	21/08/1951	09 48.05	83 52.90	M=5.0	F
17	09/09/1952	09 12.00	84 12.00	Ms=7.0	S
18	30/12/1952	10 01.50	83 54.50	M=5.5	F
19	01/09/1955	10 14.00	84 19.60	M=5.8	F
20	09/04/1966	09 12.00	84 14.40	Mb=5.3	S
21	05/08/1971	09 12.60	84 15.00	Mb=5.0	S
22	04/08/1973	09 27.60	84 51.60	Mb=5.1	S
23	25/11/1976	09 25.80	84 52.80	Mb=5.1	S
24	01/12/1976	09 27.00	84 55.90	Mb=5.3	S
25	17/08/1982	09 12.60	84 14.40	Mb=5.4	S
26	03/07/1983	09 30.60	83 40.02	Ms=6.2	F
27	25/09/1985	09 02.63	84 02.57	Mb=5.2	
28	31/01/1988	09 47.24	83 47.68	Mb=5.4	
29	02/03/1988	09 31.77	84 52.30	Mb=5.5	
30	26/02/1989	09 38.97	84 13.26	Mb=5.4	
31	25/03/1990	09 35.17	84 56.26	Mb=6.5	
32	25/03/1990	09 32.53	84 56.66	Mb=5.7	
33	30/06/1990	09 49.50	84 22.86	Mb=5.4	
34	23/07/1990	09 20.24	84 47.61	Mb=5.5	
35	22/12/1990	09 54.66	84 18.77	Mb=5.9	

* Fuentes: F = Falla, S = Proceso de subduccion

Table 8-4 Annual Number of Earthquakes during 1900-1992

$D \leq 1,000$ km ($D =$ Epicentral Distance)

Year	N	Sum of N	Year	N	Sum of N
1902	2	2	1952	17	216
1904	5	7	1953	5	221
1905	1	8	1954	11	232
1906	2	10	1955	8	240
1907	1	11	1956	12	252
1909	1	12	1957	9	261
1910	4	16	1958	7	268
1911	1	17	1959	9	277
1912	3	20	1960	10	287
1913	1	21	1961	11	298
1914	2	23	1962	11	309
1915	2	25	1963	98	407
1916	6	31	1964	170	577
1919	3	34	1965	164	741
1920	2	36	1966	147	888
1921	4	40	1967	140	1028
1924	7	47	1968	80	1108
1925	5	52	1969	95	1203
1926	6	58	1970	113	1316
1927	2	60	1971	75	1391
1929	2	62	1972	87	1478
1930	1	63	1973	132	1610
1931	10	73	1974	187	1797
1932	5	78	1975	115	1912
1933	11	89	1976	239	2151
1934	14	103	1977	106	2257
1935	5	108	1978	114	2371
1936	2	110	1979	214	2585
1937	6	116	1980	141	2726
1939	13	129	1981	112	2838
1940	5	134	1982	169	3007
1941	12	146	1983	139	3146
1942	7	153	1984	128	3274
1943	5	158	1985	140	3414
1944	3	161	1986	123	3537
1945	5	166	1987	203	3740
1946	3	169	1988	11	3751
1947	2	171	1989	9	3760
1948	3	174	1990	58	3818
1949	2	176	1991	54	3872
1950	9	185	1992	14	3886
1951	14	199			

Table 8-5 Distribution of Magnitude and Epicentral Distance of Earthquakes during 1900-1992

DISTRIBUTION OF MAGNITUDE AND EPICENTRAL DISTANCE OF THE SEISMICITY DATA

	0<=D<50	50<100	100<200	200<300	300<400	400<500	500<600	600<700	700<800	800<1000	1000<=	TOTAL
0<M<3.0	0	0	0	0	0	0	0	0	0	0	0	0
<3.5	0	0	0	0	0	1	0	0	0	0	0	1
<4.0	0	2	8	2	7	5	17	12	16	77	0	146
<4.5	20	52	101	59	74	63	100	110	170	351	0	1100
<5.0	29	50	115	89	138	101	136	183	217	540	0	1598
<5.5	17	18	48	30	57	44	44	64	73	200	0	595
<6.0	5	5	21	9	15	13	8	9	10	46	0	141
<6.5	2	1	8	16	17	14	12	12	12	41	0	135
<7.0	4	10	14	9	13	13	9	7	7	29	0	115
<7.5	2	5	11	3	3	5	0	4	6	4	0	43
<8.0	0	0	4	1	0	0	0	0	0	4	0	9
8.0<=	0	0	1	0	0	0	0	0	0	2	0	3
UNKNOWN	0	0	0	0	0	0	0	0	0	0	0	0
TOTAL	79	143	331	218	324	259	326	401	511	1294	0	3886

D : EPICENTRAL DISTANCE (KM)
M : MAGNITUDE

Table 8-6 (1) Annual Maximum Accelerations during 1900-1992

YEAR	ATTENUATION MODEL			
	OLIVEIRA	MCGUIRE	ESTEVA & ROSENBLUTH	KATAYAMA
1900	0.0	0.0	0.0	0.0
1901	0.0	0.0	0.0	0.0
1902	0.69	9.16	0.99	4.20
1903	0.0	0.0	0.0	0.0
1904	25.46	102.89	23.28	92.29
1905	34.85	104.09	32.00	71.10
1906	0.78	10.44	1.16	5.23
1907	2.09	17.39	2.28	8.43
1908	0.0	0.0	0.0	0.0
1909	27.84	92.91	24.67	65.17
1910	3.98	21.95	3.54	8.82
1911	5.04	25.60	4.45	10.65
1912	5.94	28.48	5.23	12.12
1913	1.20	11.31	1.33	4.54
1914	0.70	8.56	0.91	3.49
1915	0.84	10.14	1.12	4.60
1916	34.35	110.84	30.37	85.41
1917	0.0	0.0	0.0	0.0
1918	0.0	0.0	0.0	0.0
1919	1.94	15.71	2.04	6.96
1920	1.49	12.71	1.56	5.09
1921	1.30	12.86	1.54	5.85
1922	0.0	0.0	0.0	0.0
1923	0.0	0.0	0.0	0.0
1924	86.20	192.42	94.15	152.52
1925	1.96	16.11	2.09	7.35
1926	1.87	15.80	2.03	7.32
1927	0.99	10.53	1.19	4.43
1928	0.0	0.0	0.0	0.0
1929	1.93	15.05	1.95	6.28
1930	0.56	6.89	0.70	2.44
1931	2.01	15.45	2.02	6.49
1932	1.97	16.18	2.10	7.38
1933	3.40	21.77	3.22	9.91
1934	6.06	36.06	5.93	21.84
1935	0.67	7.75	0.81	2.82
1936	4.29	24.60	3.92	11.06
1937	16.90	63.70	14.91	38.29
1938	0.0	0.0	0.0	0.0
1939	33.72	109.52	29.80	84.19
1940	59.32	142.58	64.83	97.89
1941	13.92	61.65	12.33	43.28
1942	0.93	9.40	1.05	4.20
1943	0.94	10.26	1.15	4.33
1944	1.18	10.93	1.28	4.22
1945	6.45	35.64	6.04	20.09
1946	0.27	4.31	0.38	1.39
1947	1.60	14.62	1.82	6.80
1948	16.41	65.42	14.48	42.21
1949	6.55	34.65	5.98	18.47
1950	12.10	58.99	11.32	42.34
1951	1.31	12.60	1.51	5.54
1952	49.05	132.06	46.74	96.60
1953	0.38	5.76	0.55	2.16
1954	1.21	11.65	1.37	4.86

Table 8-6 (2) Annual Maximum Accelerations during 1900-1992

YEAR	ATTENUATION MODEL			
	OLIVEIRA	MCCUIRE	ESTEVA & ROSENBLUETH	KATAYAMA
1955	10.71	43.35	9.48	21.19
1956	26.97	83.76	25.04	50.80
1957	6.55	34.65	5.98	18.47
1958	6.38	34.70	5.90	18.95
1959	1.78	14.73	1.87	6.34
1960	2.14	16.89	2.23	7.70
1961	9.12	39.47	8.03	19.22
1962	5.05	29.82	4.78	15.72
1963	4.68	21.38	4.22	7.07
1964	8.24	30.14	8.46	10.22
1965	6.70	26.35	6.53	8.97
1966	21.00	66.38	20.22	34.57
1967	1.64	12.80	1.62	4.77
1968	3.47	19.14	3.07	6.99
1969	17.80	50.97	24.12	19.54
1970	5.96	24.71	5.59	8.24
1971	22.01	66.02	22.78	32.40
1972	5.23	26.25	4.62	10.97
1973	14.67	53.66	14.52	30.96
1974	21.88	69.00	20.91	36.89
1975	4.46	20.72	4.01	6.81
1976	22.82	66.77	24.54	32.18
1977	6.33	27.63	5.66	10.51
1978	28.75	95.22	25.48	67.48
1979	10.60	44.66	9.63	23.15
1980	8.64	32.23	8.44	11.72
1981	5.69	24.58	5.20	8.50
1982	16.93	55.66	16.39	26.52
1983	23.01	72.15	21.87	39.64
1984	13.60	44.90	14.07	18.33
1985	14.66	49.47	14.24	22.21
1986	3.92	20.19	3.45	7.18
1987	12.52	41.54	13.27	16.09
1988	18.75	57.37	19.91	25.91
1989	5.15	23.32	4.62	8.58
1990	77.06	170.27	92.43	121.68
1991	21.33	78.43	25.05	53.40
1992	21.62	55.13	48.50	19.49

Table 8-7 Maximum Accelerations for Six Return Periods

(Unit: gal)

Attenuation Model	Return Period (Year)					
	50	100	200	500	1000	10000
(1) C. Oliveira	64.5	81.9	99.2	120.8	135.6	173.6
(2) R.K. McGuire	157.8	185.8	211.7	242.3	262.2	310.3
(3) Esteva & Rosenblueth	70.6	89.6	108.4	131.5	147.2	186.6
(4) T. Katayama	125.3	148.7	169.2	191.8	205.4	234.3

Chapter 9 Development Plan

Chapter 9 Development Plan

CHAPTER 9 DEVELOPMENT PLAN

Contents

9.1	Review of Existing Development Plans.....	9-1
9.1.1	General Outline.....	9-1
9.1.2	Estimation of Electric Energy Generation.....	9-3
9.1.3	Selection of the Project Site.....	9-4
9.2	Basic Development Plan.....	9-5
9.2.1	Basic Conditions for Study.....	9-5
9.2.2	Comparison Studies of Development Plan.....	9-6
9.2.3	Basic Development Plan.....	9-8
9.3	Optimum Development Plan.....	9-9
9.3.1	Downstream Effects upon the Naranjo River caused by Development Plan.....	9-9
9.3.2	Studies of Maximum Discharge.....	9-10
9.3.3	Comparison Study of Major Structures.....	9-11
9.3.4	Optimum Development Plan.....	9-14

List of Figures

- Fig. 9-1 Naranjo River Master Plan Layout
- Fig. 9-2 Los Llanos Alternative Layout
- Fig. 9-3 Reservoir Operation at Los Llanos (2)
- Fig. 9-4 Study on Reservoir Storage Volume at Los Llanos
- Fig. 9-5 Los Llanos Dam (Case II-2) Plan and Sections
- Fig. 9-6 Tocori Supply Water Facilities Plan and Sections
- Fig. 9-7 (1) Area - Capacity Curve 1/2
- Fig. 9-7 (2) Area - Capacity Curve 2/2
- Fig. 9-8 Los Llanos Dam Cross Section of Alternative Dam Site
- Fig. 9-9 Cross Section ~ Dam Height
- Fig. 9-10 Headrace Tunnel Layout
- Fig. 9-11 Penstock Alternative Layout
- Fig. 9-12 (1) Profile of Penstock Open Type
- Fig. 9-12 (2) Profile of Penstock Tunnel Type
- Fig. 9-13 General Plan
- Fig. 9-14 Los Llanos Dam Plan and Section
- Fig. 9-15 Study on Maximum Discharge

List of Tables

Table 9-1	Project Outline of Naranjo River Basin
Table 9-2	Estimation of Electric Energy Generation
Table 9-3 (1)	Energy Production of Los Reyes Scheme
Table 9-3 (2)	Energy Production of Milagro Scheme
Table 9-3 (3)	Energy Production of Los Llanos Scheme
Table 9-3 (4)	Energy Production of Los Llanos Scheme (A)
Table 9-3 (5)	Energy Production of Nara Scheme
Table 9-4	Study of Project Site
Table 9-5	Project Outline of Los Llanos Scheme
Table 9-6	Basic Development Plan of Los Llanos Project
Table 9-7	Project Outline of Los Llanos Projects
Table 9-8 (1)	Energy Production of Los Llanos Scheme (1)
Table 9-8 (2)	Energy Production of Los Llanos Scheme (2)
Table 9-8 (3)	Energy Production of Los Llanos Scheme (3)
Table 9-8 (4)	Energy Production of Los Llanos Scheme (4)
Table 9-9	Investment Cost
Table 9-10	Basic Development of Los Llanos Project
Table 9-11	Monthly Average Inflow at the Intake Channel Site (without Project)
Table 9-12	Monthly Average Inflow at the Intake Channel Site (with Project)
Table 9-13 (1)	Outline of Los Llanos Project (I)
Table 9-13 (2)	Outline of Los Llanos Project (II)
Table 9-14	Development Plan of Los Llanos Project
Table 9-15	Study on Turbine Type
Table 9-16	Standard Alternative Thermal Power Plant
Table 9-17	Result of Optimum Development Plan

CHAPTER 9 DEVELOPMENT PLAN

9.1 Review of Existing Development Plans

9.1.1 General Outline

The Naranjo River originates in Mt. Cruce Chinchilla in Province of San Jose, 2,984 m above sea level. After joined by the Naranjillo River in the upstream and the Brujo River in the middle course, it flows rapidly down to the boundary with Province of Puntarenas, then flows through flat terrain to the Pacific. The river has catchment area of 332 km² and is 41 km long.

The catchment area of the Naranjo River belongs to tropical rainy climate. Annual precipitation exceeds 6,000 mm in the mountainous upper stream area, and more than 4,000 mm in the downstream flat area. Gradient is around 1/20. These make the river ideally suitable for hydropower generation.

At present, five hydropower projects are proposed for the Naranjo River basin under "Plan Maestro de la Cuenca Hidrografia Rio Naranjo." They are, as shown in Fig. 9-1, Reyes Project, Milagro Project, Los Llanos Project, Los Llanos-A Project, and Nara Project. Major features of these projects are summarized in Table 9-1. Their general outline is as follows.

(1) Reyes Project

Reyes Project envisages to build a 113 m high rock-fill dam in the Naranjillo River, a branch of the Naranjo River, having catchment area of 68.0 km². Using water depth of 40 m created by H.W.L. 880 m and L.W.L. 840 m, the dam will have effective storage capacity of 23.8×10^6 m³. Water will be collected through an intake on the left side of the dam at maximum rate of 10.8 m³/s and will be directed through a 3,600 m long headrace tunnel (inner diameter of 2.4 m) and a 600 m long penstock (inner diameter of 1.5 m) to a power plant to be constructed on the left side of the downstream of the Naranjillo River. With effective head of 255 m, the plant will generate maximum output of 23.3 MW. Water will then be discharged through a tailrace to the Naranjillo River.

(2) Milagro Project

The project will construct a 10 m high intake dam in the upstream of the Naranjo River to cover catchment area of 27.0 km². Through an intake built on the right bank of the dam, water will be taken in at maximum rate of 6.3 m³/s and will flow through a 4,000 m headrace tunnel (inner diameter of 2.4 m) and a 1,100 m penstock (inner diameter of 1.2 m), down to a power plant (effective head of 577 m, and maximum output of 30.8 MW) to be built on the right side of the downstream of the Naranjo River. Finally it will be discharged through a tailrace to the Naranjo River.

(3) Los Llanos Project

A 53 m high concrete gravity dam will be constructed in the downstream of a confluence of the Naranjo and Naranjillo Rivers, with catchment area of 143.7 km². The dam will have effective storage capacity of 1.5 x 10⁶ m³ by using water depth of 10 m between H.W.L. 485 m and L.W.L. 475 m. Water will be collected through an intake on the right side of the dam at maximum rate of 31.0 m³/s, and will be led through a 5,900 m headrace tunnel (inner diameter of 3.2 m) and a 1,465 m penstock (inner diameter of 2.75 m) to a power plant on the left side of the Paquita River (effective head of 365 m, and maximum output of 95.8 MW), followed by discharge to the Paquita River through a tailrace.

(4) Los Llanos-A Project

The project is basically same as Los Llanos Project up to the dam. It will construct a 53 m high concrete gravity dam in the downstream of a confluence of the Naranjo river and the Naranjillo river, with catchment area of 143.7 km². The dam will have effective storage capacity of 1.5 x 10⁶ m³ by using water depth of 10 m between H.W.L. 485 m and L.W.L. 475 m. Water will then be collected through an intake on the right side of the dam at maximum rate of 31.0 m³/s, and will be led through a 2,400 m headrace tunnel (inner diameter of 3.2 m) and a 1,160 m penstock (inner diameter of 2.75 m) to a power plant to be built on the right side of the Naranjo river (effective head of 167 m, and maximum output of 43.7 MW). Finally, water will be discharged through a tailrace to the Naranjo River.

(5) Nara Project

A 10 m high intake dam will be constructed in the Brujo River, a branch of the Naranjo River, with catchment area of 28.0 km². Through an intake to be built on the left side of

the dam, water will be collected at maximum rate of 6.2 m³/s and will be led through a 2,800 m headrace tunnel (inner diameter of 2.4 m) and a 1,550 m penstock (inner diameter of 1.2 m) to a power plant on the left side of the Savegre River (effective head of 432 m and maximum output of 22.7 MW). Finally, water will be discharged through a tailrace to the Savegre River.

9.1.2 Estimation of Electric Energy Generation

Based on discharge at the proposed points, this section estimates effective output and electric energy production from each project as shown in Table 9-2.

The following assumptions are made to determine effective output and electric energy to be used for reviewing of the master plan.

(1) Effective Output

The proposed plant is assumed to have the ability to generate electricity continuously for more than six hours each on 355 days or more in a year. Data used are the mean value of discharge over 23 years between 1971 through 1993.

(a) Run-of-River Type (Milagro and Nara Projects)

Average output for 355-day flow rate

- Generation efficiency of 0.84.
- Effective head is assumed to be the one to achieve maximum output.

(b) Daily Regulating Pondage Type (Los Llanos and Los Llanos-A Projects)

Peak output for 355-day flow rate

- Generation efficiency of 0.84.
- Effective head is assumed to be the one to achieve maximum output.

(c) Reservoir Type (Los Reyes)

Water stored during the wet season, up to the effective storage capacity, will be supplied during the dry season (principally December through April) at a rate required to maintain daily average water consumption for power generation at a maximum and constant level.

Peak output for 355-day flow rate

- Generation efficiency of 0.84.
- Effective head is the head obtained when the intake level is assumed to be the highest level less one third of the available water level.

(2) Effective Electric Energy Production

Effective electric energy production is assumed to be the average amount of electric energy that can be generated in a year. Note that the same generation efficiency and effective head are assumed.

(a) Run-of-River and Daily Regulating Pondage Types

Calculated by multiplying river runoff up to the maximum discharge by generation efficiency and effective head.

(b) Reservoir Type

The value obtained in (a) above is added by the water volume stored during the wet season, up to the effective storage capacity, which is then multiplied by generation efficiency and effective head.

9.1.3 Selection of the Project Site

Preliminary costs of the five projects, Reyes, Milagro, Los Llanos, Los Llanos-A, and Nara, are estimated. Note that work quantities have been estimated on the basis of the projects completed in the past, and unit costs have been determined on the basis of those indicated in the Feasibility Study Report of Pirris Project (as of 1991). These costs do not include compensation and construction of transmission lines. Based on project cost, firm power, and annual available energy estimated for each project site as shown in Tables 9-3 (1) to 9-3 (5), benefit cost ratio (B/C) and unit cost of energy (c/kWh) have been determined for the projects and compared in Table 9-4. Among the five projects, Los Llanos show the best B/C and c/kWh, same as the result indicated in Master Plan. Note that benefits have been estimated on the basis of kW cost of 119.57 \$/kWh and 0.03 \$/kWh obtained in the Feasibility Study Report of Pirris Project.

9.2 Basic Development Plan

9.2.1 Basic Conditions for Study

The following conditions are made to determine effective output and electric energy to be used for study of Los Llanos Project site.

(1) Effective Output

The proposed plant is assumed to have the ability to generate electricity continuously for more than five hours each on 332 days (95%) or more in a year. Data used are the mean value of discharge over 23 years between 1971 through 1993.

(a) Daily regulating pondage type (Los Llanos (1), (A) and (B) projects)

Peak output for 332-day flow rate

- Generation efficiency of 0.84.
- Effective head is assumed to be the one to achieve maximum output.

(b) Reservoir type (Los Llanos (2), Los Llanos (3), and Los Llanos (4))

Water stored during the wet season, up to the effective storage capacity, will be supplied during the dry season (principally December through April) at a rate required to maintain daily average water consumption for power generation at a maximum and constant level.

Peak output for 332-day flow rate

- Generation efficiency of 0.84.
- Effective head is the head obtained when the intake level is assumed to be the highest level less one third of the available water level.

(2) Effective Electric Energy Production

Effective electric energy production is assumed to be the average amount of electric energy that can be generated in a year. Note that the same generation efficiency and effective head are assumed.

(a) Daily regulated pondage types

Calculated by multiplying river runoff up to the maximum discharge by generation efficiency and effective head.

(b) Reservoir type

The value obtained in (a) above is added by the water volume stored during the wet season, up to the effective storage capacity, which is then multiplied by generation efficiency and effective head.

9.2.2 Comparison Studies of Development Plan

For Los Llanos hydroelectric power development plan, three projects are proposed; Los Llanos, Los Llanos (A), and Los Llanos (B) as shown in Fig. 9-2.

Major features of these projects are summarized in Table 9-5. Their general outline is as follows.

Los Llanos Project

A 53 m high concrete gravity dam will be constructed in the downstream of a confluence of the Naranjo and Naranjillo Rivers, with catchment area of 143.7 km². The dam will have effective storage capacity of 1.5×10^6 m³ by using water depth of 10 m between H.W.L. 485 m and L.W.L. 475 m. Water will be collected through an intake on the right side of the dam at maximum rate of 31.0 m³/s, and will be led through a 5,900 m headrace tunnel (inner diameter of 3.2 m) and a 1,465 m penstock (inner diameter of 2.75 m) to a power plant on the left side of the Paquita River (effective head of 365 m, and maximum output of 95.8 MW), followed by discharge to the Paquita River through a tailrace.

Los Llanos (A) Project

The project is basically same as Los Llanos Project up to the dam. It will construct a 53 m high concrete gravity dam in the downstream of a confluence of the Naranjo River and the Naranjillo River, with catchment area of 143.7 km². The dam will have effective storage capacity of 1.5 x 10⁶ m³ by using water depth of 10 m between H.W.L. 485 m and L.W.L. 475 m. Water will then be collected through an intake on the right side of the dam at maximum rate of 31.0 m³/s, and will be led through a 2,400 m headrace tunnel (inner diameter of 3.2 m) and a 1,160 m penstock (inner diameter of 2.75 m) to a power plant to be built on the right side of the Naranjo River (effective head of 167 m, and maximum output of 43.7 MW). Finally, water will be discharged through a tailrace to the Naranjo River.

Los Llanos (B) Project

The project is basically same as Los Llanos Project up to the dam. It will construct a 53 m high concrete gravity dam in the downstream of a confluence of the Naranjo River and the Naranjillo River, with catchment area of 143.7 km². The dam will have effective storage capacity of 1.5 x 10⁶ m³ by using water depth of 10 m between H.W.L. 485 m and L.W.L. 475 m. Water will then be collected through an intake on the left side of the dam at maximum rate of 31.0 m³/s and an intake in the Brujo River at maximum rate of 9.0 m³/s and will be led through a 5,300 m and a 2,400 m headrace tunnel (inner diameter of 3.2 m and 3.6 m) and a 2,100 m penstock (inner diameter of 3.0 m) to a power plant to be built on the left side of the Naranjo River (effective head of 242 m, and maximum output of 82 MW). Finally, water will be discharged through a tailrace to the Naranjo River.

(I) Selection of the Project

Based on project cost, firm power, and annual available energy estimated for each project site, benefit cost ratio (B/C) and unit cost of energy (c/kWh) have been determined for the projects and compared in Table 9-6.

Among the three projects, Los Llanos shows the best B/C and c/kWh. Note that benefits have been estimated on the basis of kW cost of 119.57 \$/kW and 0.0373 \$/kWh for firm energy and 0.0235 \$/kWh for secondary energy obtained in the Feasibility Study Report of Pirris Project.

(2) Examination of Development Scale

In comparing the three development projects (Los Llanos (1), Los Llanos (A), and Los Llanos (B)), Los Llanos (1) Project has been identified as the project with the highest economic feasibility and has been further studied to determine the optimum dam size by using 4 cases of dam height, 53 m, 138 m, 108 m and 93 m. Major features for these cases are summarized in Table 9-7. Los Llanos (1) Project is assumed to be of daily regulating pondage type in consideration to effective storage capacity of $1.5 \times 10^6 \text{ m}^3$. On the other hand, Los Llanos (2), (3) and (4) Projects have effective storage capacity of $22.5 \times 10^6 \text{ m}^3$, $9.5 \times 10^6 \text{ m}^3$ and $5.0 \times 10^6 \text{ m}^3$ respectively, so that they are assumed to be of reservoir type which stores water during the wet season up to the respective effective storage capacity and supplies it during the dry season for increased effective output and electric energy as shown in Fig. 9-3.

Based on discharge at Los Llanos, monthly energy has been calculated as shown in Tables 9-8 (1) to 9-8 (4).

Then the project cost has been estimated as shown in Table 9-9. Based on project cost, firm power, and annual available energy estimated for each of Los Llanos (1), (2), (3) and (4) Projects, benefit cost ratio (B/C) and unit cost of energy (c/kWh) have been estimated and compared as shown in Table 9-10 and Fig. 9-4 respectively. The result reveals that Los Llanos (1) Project is best in terms of B/C and c/kWh.

9.2.3 Basic Development Plan

Among the six projects contemplated in development plan for the Naranjo River basin (Reyes, Milagro, Los Llanos, Los Llanos (A), Los Llanos (B) and Nara), comparative evaluation reveals that Los Llanos is the best alternative.

Then Los Llanos project site has been further studied for four cases with effective storage capacity of $1.5 \times 10^6 \text{ m}^3$, $5.0 \times 10^6 \text{ m}^3$, $9.5 \times 10^6 \text{ m}^3$, and $22.5 \times 10^6 \text{ m}^3$ respectively. The first case with effective storage capacity of $1.5 \times 10^6 \text{ m}^3$ has been found to have the highest economic feasibility study. Based on the result, a basic power source development project for the Naranjo River is to construct a 50 m high dam at Los Llanos with storage capacity allowing daily regulation. From the dam, available discharge of $31 \text{ m}^3/\text{s}$ will be diverted to the Paquita River and will be used by a power plant having effective head of 400 m and maximum output of 96 MW.

9.3 Optimum Development Plan

9.3.1 Downstream Effects upon the Naranjo River caused by Development Plan

The previous study regarding a development plan for a hydroelectric project on the Naranjo River confirmed the following: the most advisable location for the dam is at the downstream junction point of the Naranjo River and the Naranjillo River-setting up the water-intake at the right bank of the dam, guiding the water through approximately 7,000 m of waterway to the power plant to be built on the left bank of the Paquita River, and finally, discharging the water used for generating electricity into the Paquita River.

Since the plan involves two rivers (the Naranjo River and the Paquita River), it is critical to examine the downstream effects upon the Naranjo River. Therefore, an environmental-impact was studied as shown in Chapter 13.

In Puntarenas Plain downstream of the Naranjo River, the river water is used for irrigation of African palm plantations, taking in at maximum rate of $1.8 \text{ m}^3/\text{s}$ through an intake channel on the left side of the Naranjo River. The monthly average inflow at the intake channel will decrease owing to Los Llanos hydroelectric project as shown in Table 9-11 and Table 9-12.

The counter measure for securing water for irrigation is considered as follows.

- (1) The height of dam is required to be higher in order to retain an extra volume of water ($5 \times 10^6 \text{ m}^3$ at maximum rate of $1.8 \text{ m}^3/\text{s}$) to be supplied downstream in addition to the regulating capacity as shown in Fig. 9-5.
- (2) Tocorí dam is required to be constructed in order to retain an volume of water ($5 \times 10^6 \text{ m}^3$ at maximum rate of $1.8 \text{ m}^3/\text{s}$) to be supplied downstream with the attached water way as shown in Fig. 9-6.
- (3) Compensation is required to make up a poor African palm harvest owing to the decreased water caused by Los Llanos hydroelectric project. Compensation cost is 550×10^3 U.S. dollar/year as shown in Chapter 13.

9.3.2 Studies of Maximum Discharge

In order to most efficiently utilize water from the Naranjo River to meet the demand for electric power in Costa Rica, the following conditions have to be met with regard to the discharge required for hydroelectric generation at the power plant:

- (1) Firm inflow should be 95% of the inflow
- (2) Peak running time should be 5 hours
- (3) The Reservoir should be controlled with weekly adjustment (7/5)

The following is the formula to calculate the discharge for hydroelectric generation:

$$Q = Q_f \times 24/5 \times 7/5$$

In order to determine the optimum scale of the power plant, the study was conducted for four cases according to maximum discharge of 20, 25, 30, and 35 m³/s.

(1) When a supply of water downstream is not considered (CASE D)

The maximum water level of the reservoir (the projected sedimentation level at EL. 460 m, and the low-water level at EL. 470 m) is determined for each of the four cases according to the regulating capacity required for power generation as shown in Fig. 9-7.

The gate type dam is adopted in order for inflow load in the reservoir to be discharged during flooding by a flushing effect.

Table 9-13 (1) shows the projected outlines for each of the four cases. Installed capacity will be 60, 75, 90, and 105 MW, respectively. As indicated in Table 9-14, both B/C and B-C show the most economical efficiency when the output power is 75 MW.

(2) When a supply of water downstream is considered from Tocori Dam (CASE I')

Investment cost for Tocori dam with the attached water way will be added in CASE I.

As indicated in Table 9-14, CASE I' would be cost-effective, since the extra Tocori dam with the attached water way would result in a great construction cost.

(3) When a supply of water downstream is considered (CASE II)

The maximum water level of the reservoir (the project sedimentation level at EL. 496 m calculated by assuming the total sedimentation for 50 years to be $4.2 \times 10^6 \text{ m}^3$, and the low-water level at EL 506 m) is determined for each of the four cases according to the regulating capacity required for power generation, and by adding the amount of water to be supplied ($5 \times 10^6 \text{ m}^3$) downstream during the dry season as shown in Fig. 9-7.

Table 9-13 (2) shows the projected outlines for each of the four cases. Installed capacity will be 66, 83, 100, and 116 MW, respectively. The height of the dam is required to be higher in order to retain an extra volume of water ($5 \times 10^6 \text{ m}^3$) to be supplied downstream in addition to the regulating capacity required for power generation. As indicated in Table 9-14, none of the four cases would be cost-effective, since the extra height of the dam would result in extra construction costs.

9.3.3 Comparison Study of Major Structures

(1) Dam Site and Dam Type

The proposed dam sites of this Project are located at midstream of the Naranjo River. Three sites are considered by ICE, between 300 m and 700 m downstream from the confluence of the Naranjo River and the Naranjillo River. The related geological studies have been conducted.

The geological condition of the proposed dam sites is the conglomerate of the Palaeogene. Topographically, the sites are located in an extremely steep canyon. Of the three sites, the cross-sectional configuration of the upper stream dam site (hereinafter referred to as the upper stream axis) is practically symmetric, inclining 63° from the river bed to a height of 30 m against the horizontal plane. This inclination is gradual, ranging from 35° to 48° at heights from 30 m - 60 m. This becomes further gradual to 25° to 28° over a height of 60 m.

Regarding the dam site at midstream (midstream axis), the left bank forms an evenly steep slope of 58° . The right bank forms a 44° slope to a height of 40 m from where a relatively gradual slope of 38° rises.

The downstream dam site (downstream axis) appears symmetrical. The inclination of the left bank to a height of approx. 45 m is 60° , changing to 40° above that height. In

contrast, the inclination of the right bank to a height of 70 m is even with a 60° slope. This changes to a relatively gradual 60° slope above the 70 m level. The locations of the proposed dam sites and the river cross section are described in Fig. 9-8.

The relation between the dam height and cross sectional area is shown in Fig. 9-9. According to Fig. 9-9, the downstream axis requires the least dam volume. Therefore, the downstream axis is the most suitable dam site for the development plan. As because the crest length and height ratio (L/H) is 1.7, the most suitable types of dam are the concrete arch type and the concrete gravity type. In the comparison study for this development project the subject was limited to a concrete gravity dam for the following reasons;

- a) Insufficient geological study.
- b) The geological conditions at the right bank provide some problems for a high crest.

(2) Headrace Route

Considering the location and the length of headrace including work adit, three routes are available. Two plans are available for the work adit; the adit from Queb. Lagartijo (Rio Naranjo side) to the headrace, and the adit from Queb. Jilguero (Rio Paquita). Comparing these two plans, the Queb. Jilguero plan is appropriate for the following reasons;

- 1) Construction of an access road from the existing road to the work adit is easy.
- 2) The topography is suitable for installing the concrete plant and other temporary facilities.

Each headrace route is shown in Fig. 9-10. The extension of each plan is described below. Comparing the construction costs, Route-2 provides the best economic route.

Route	Headrace Tunnel (m)	Work Adit (m)	Total Length (m)
Route-1	5,593	448	6,041
Route-2	5,612	193	5,805
Route-3	5,648	380	6,028

The concrete thickness for the headrace tunnel in the standard area is 30cm. Assuming that 25% of the entire section provides poor geological conditions, the concrete thickness is determined at 50cm for that area. For approx. 20m immediately under Adit-B where the tunnel is covered with thin soil, a 10mm thick steel liner is applied for reinforcement.

Initially, the construction of a 5,540m long tunnel was planned with 2 work adits. Due to a 12m head between the intake and headrace tunnel, however, the work from the intake may be delayed. Therefore, another work adit is added, resulting in a total of three work adits. These work adits will be closed with concrete upon completion of construction.

(3) Power Plant Site and Penstock Route

The power plant site is located at the left bank downstream of the Paquita River. ICE studies both the upperstream and downstream sites as proposed plant sites. In the upperstream plan, the plant site is located at the left bank on the tributary of the Paquita River. The foundation is conglomerate.

In the downstream plan, the plant site is located on the river terrace approx. 200 m downstream from the site of the upperstream plan. Here, the foundation is conglomerate and marl. The conglomerate lies above the marl. ICE considers that being supported by conglomerate, the upperstream site is more appropriate than the downstream site where due to the marl, deterioration after excavation may be faster.

However, our last on-site survey and ICE's additional boring indicates that the marl can retain adequate supportive strength when its surface is protected with an appropriate material such as mortar or concrete after excavation. Therefore, the downstream site is selected as the plant site due to the easy access and the convenience provided for the construction of related facilities. The final plant location will be determined based on the penstock route.

The topography of the penstock location provides a gentle slope at the highest level, and increases its inclination gradually from the medium high level to the lower levels. The average inclination is gradual at 14° but varies at the medium height levels. The foundation of the penstock is conglomerate and is, therefore, firm. The surface bed is deep at 9 m - 14 m.